Supplementary Materials

Whole-ecosystem experiments reveal varying responses of phytoplankton functional groups to epilimnetic mixing in a eutrophic reservoir

M.E. Lofton, R.P. McClure, S. Chen, J.C. Little, C.C. Carey

Number of pages: 12

Number of text supplements: 1

Number of tables: 1

Number of figures: 8

Text S.1. Epilimnetic mixing system and mixing experimental design

The Epilimnetic Mixing (EM) system is comprised of an onshore air compressor coupled to a distribution header located in the reservoir. The onshore compressed air system includes an air compressor (Kaeser, VA, USA), an air receiving tank, a refrigerated dryer (Dominion Air, Roanoke, VA, USA) and a mass flow controller (model MCR-100SLPM-D-I-485, Alicat Scientific, Tucson, AZ, USA). The compressed air is fed to the receiving tank and through the mass flow controller at the desired feed rate to the distribution header in the reservoir.

The distribution header is similar to diffusers used for linear bubble-plume hypolimnetic oxygenation systems, [*Singleton et al*., 2007, *Gantzer et al*., 2009]. The EM system is a two-pipe system tethered to anchors to suspend the distribution header at a depth of five meters below the water surface when the reservoir is at full pond. The three parts of the distribution header are the buoyancy pipe, supply pipe, and porous hose. The buoyancy pipe can be filled with either water or air and is used for buoyancy control to deploy and service the EM system. The supply pipe provides the compressed air and is connected to the porous hose via saddle ties along the length of the diffuser.

The EM has both active and subsequent inactive sections of porous hose. This strategy delivers compressed air at the desired gas flow rate to the furthest upstream location in the reservoir (Fig. 1). Without the active/inactive sections, the active mixing would be isolated to a small region in the deepest part of the reservoir. Compressed air is fed from the onshore compressor through 207 m of supply pipe before reaching the distribution header in the reservoir. The distribution header then continues for another 230 m, alternating between 27 m sections of porous hose and 23 m inactive sections, for a total of five active mixing sections.

The duration and flow rate of the two epilimnetic mixing events were chosen to preserve thermal stratification, as required by the managers. The two events were designed to be complementary, using different flow rates and durations to achieve the same change in metalimnetic boundary depth (a decrease of ~ 1 to 1.3 m) during both experiments. To do this, we used an empirical equation for predicting metalimnetic boundary depth under epilimnetic mixing in FCR during summer periods as a function of mixing flow rate and duration of operation developed by Chen et al. (2017):

$$h = (h_0 - 0.63{Q_{\mathrm{EM}}}^{0.21})e^{0.04t} + 0.63{Q_{\mathrm{EM}}}^{0.21}e^{-1.72{Q_{\mathrm{EM}}}^{0.24}t} \quad \text{EQ S1}$$

where h_o is the initial metalimnetic boundary measured as depth from the surface, h is the final metalimnetic boundary at time t (days of EM operation), and Q_{EM} is the EM flow rate in SCFM (Chen et al., 2017). While equation S1 predicted similar changes in the lower metalimnetic boundary after EM1 and EM2 of ~ 1 – 1.3 m, the decrease in lower metalimnetic boundary after EM2 was only 0.4 m, which may indicate that other factors such as stratification strength or seasonal temperature may need to be considered when predicting mixing effects on lower metalimnetic boundary.

Table S.1: Morphological-based functional group (MBFG) classifications of all genera identified in Falling Creek Reservoir (FCR) and Beaverdam Reservoir (BVR) during the monitoring period. MBFG classifications were based on Kruk and Segura (2012). The symbol ^ denotes morphological groups too small for further identification; filaments were ~10 μm in length; small nanophytoplankton and small nanoflagellates were 2.5-5 μm in maximum linear dimension. An asterisk denotes a genus that was classified differently in FCR and BVR based on differences in morphology such as maximum linear dimension; for these taxa, the first reported MBFG classification listed is for FCR, and the second is for BVR.

Genus	MBFG	Reservoir where present
Ankistrodesmus	4	FCR, BVR
Asterionella	6	FCR
Bacillaria	6	FCR
Carteria	1	FCR
Centritractus	1,4*	FCR, BVR
Chlamydomonas	5	FCR, BVR
Chlorella	1	FCR
Chlorgonium	5	FCR, BVR
Chromulina	5	FCR
Chroomonas	1	FCR
Closterium	1	FCR
Coccomyxa	7	FCR
Cosmarium	4	FCR, BVR
Cryptomonas	5	FCR, BVR
Cymatopleura	6	FCR
Dictyosphaerium	7	FCR, BVR
Dinobryon	5	FCR, BVR
Dolichospermum	3	FCR, BVR
Eudorina	5	FCR
filaments^	1	FCR, BVR
Gloeochaete	7	FCR
Golenkinia	1,4*	FCR, BVR
Gomphonema	6	FCR
Goniochloris	1	FCR
Gymnodinium	2	FCR
Mallomonas	5	FCR, BVR
Mesostigma	5	FCR
Microcystis	1,7*	FCR, BVR
Microspora	1	FCR
Monomorphina	5	FCR
Nephroselmis	5	FCR, BVR
Nitzchia	6	FCR
Oocystis	1,7*	FCR, BVR
Peridinium	2	FCR, BVR
Phacus	5	FCR, BVR
Phormidium	4	FCR, BVR
Small nanophytoplankton (oblong)^	1	FCR, BVR
Small nanophytoplankton (round)^	1	FCR, BVR

Small nanoflagellates (round)^	5	FCR, BVR
Pseudanabaena	4	FCR, BVR
Pyramimonas	5	FCR
Rhodomonas	5	FCR
Selenastrum	4,1*	FCR, BVR
Spondylosium	4	FCR
Synechococcus	1	FCR
Synedra	6	FCR, BVR
Synura	2	FCR, BVR
Tabellaria	6	FCR
Tetraselmis	5	FCR, BVR
Trachelomonas	2	FCR, BVR
Volvox	1	FCR
Volvulina	1	FCR

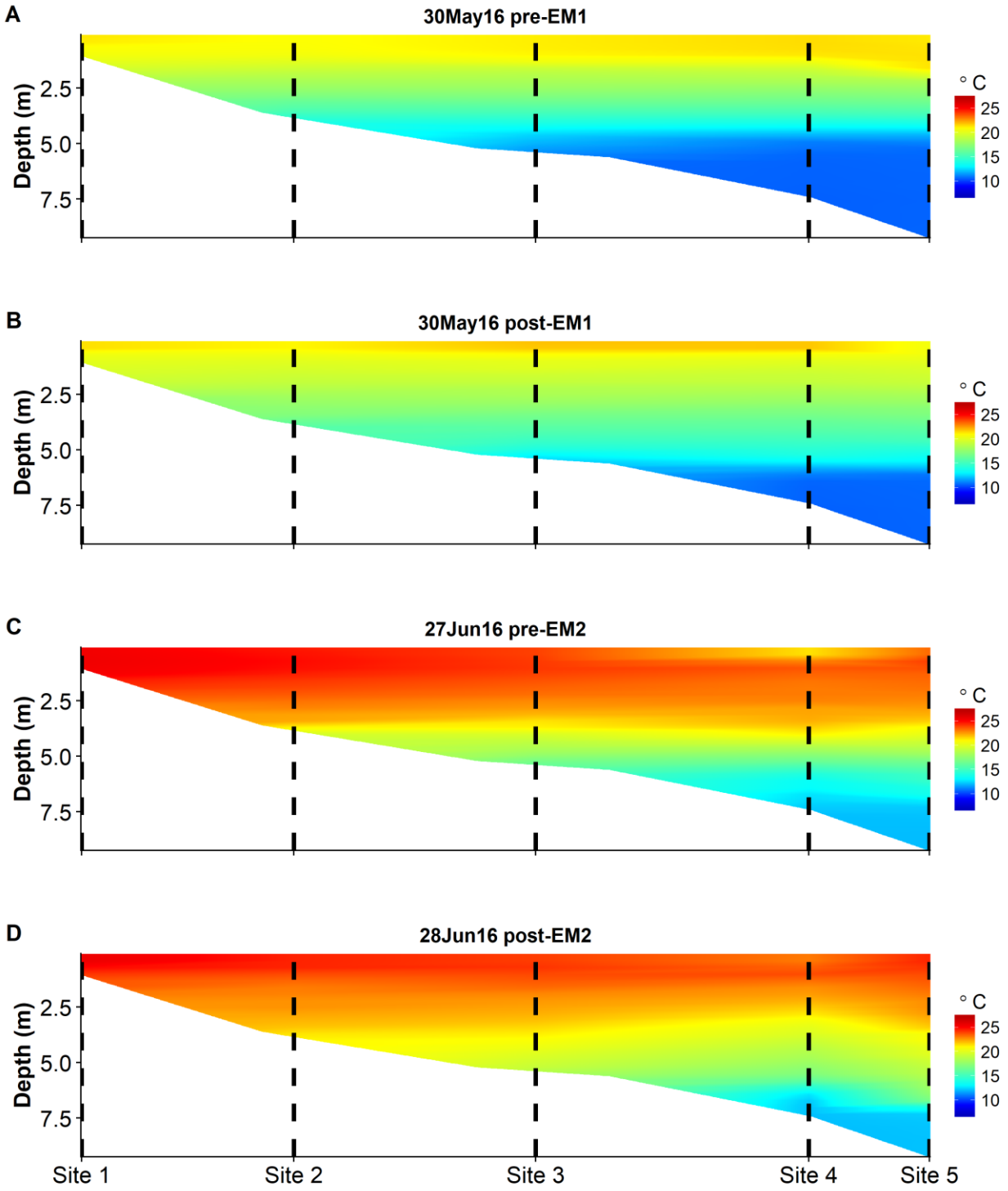

Figure S.1: Temperature across a longitudinal cross-section in Falling Creek Reservoir (FCR) from immediately before EM1 (A, 30 May 2016), immediately after EM1 (B, 30May 2016), immediately before EM2 (C, 27 June 2016) and immediately after EM2 (D, 28 June 2016). Contours are interpolated from CTD casts taken at the upstream and deepest sites (denoted by the vertical lines; upstream sampling sites are shown on the inset in Fig. 1).

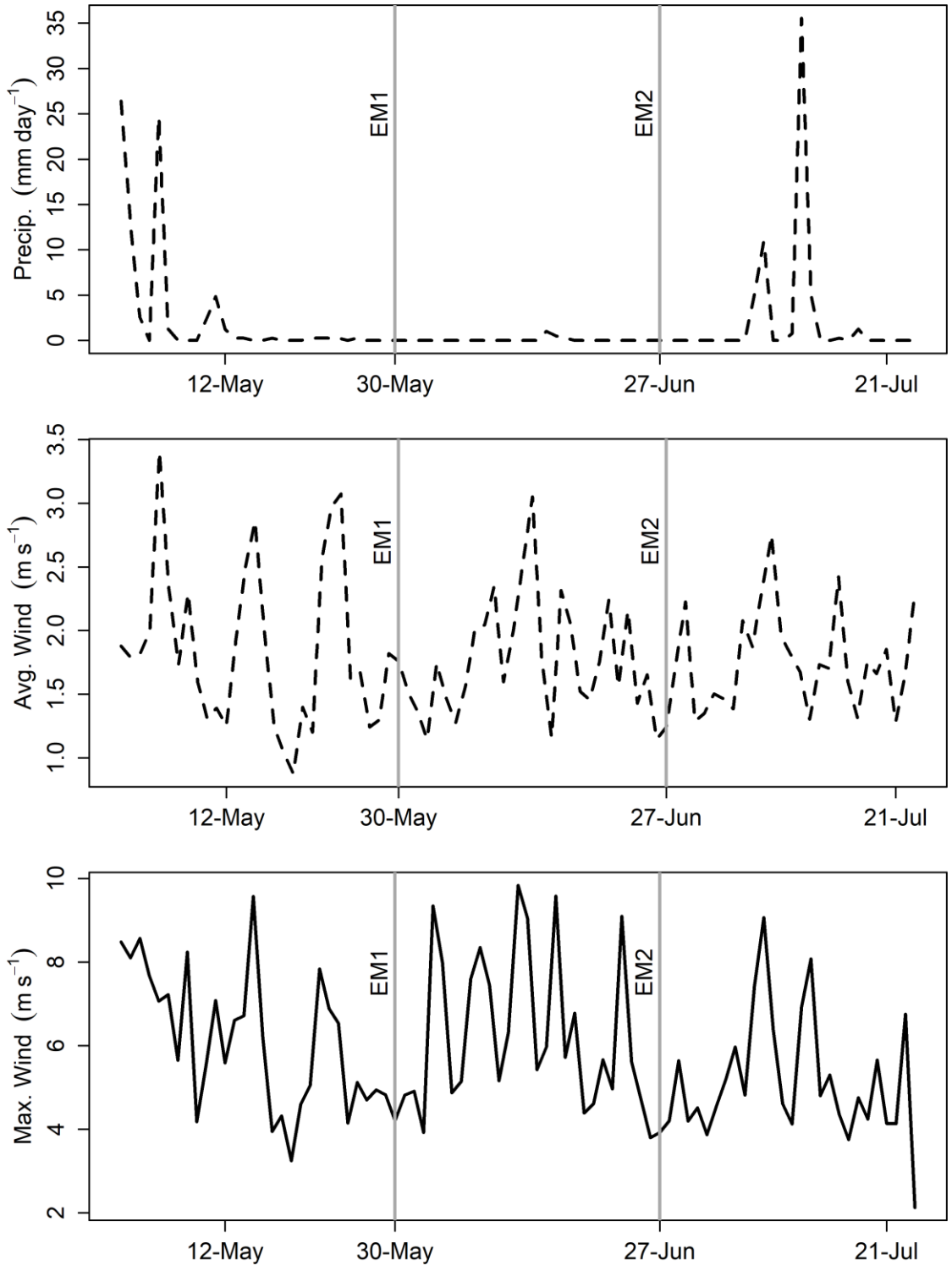

Figure S.2: Precipitation (top), daily mean wind speed (middle), and daily maximum wind speed (bottom) measured at the dam of Falling Creek Reservoir during the mixing experiments, EM1 and EM2. Mixing events are denoted by the vertical gray lines.

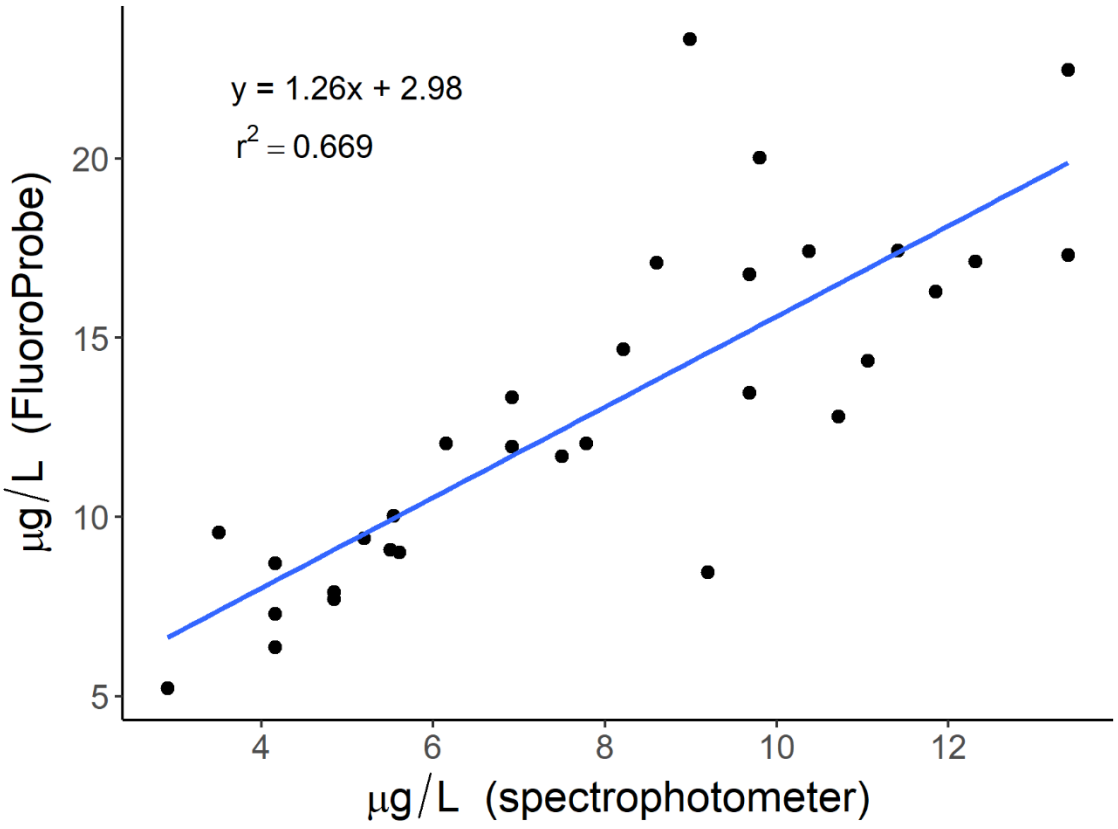

Figure S.3: Regression of total phytoplankton biomass as reported by the bbe moldaenke FluoroProbe against chlorophyll-*a* concentrations as measured using standard methods on a spectrophotometer for point samples in the epilimnia of FCR and BVR during the study period.

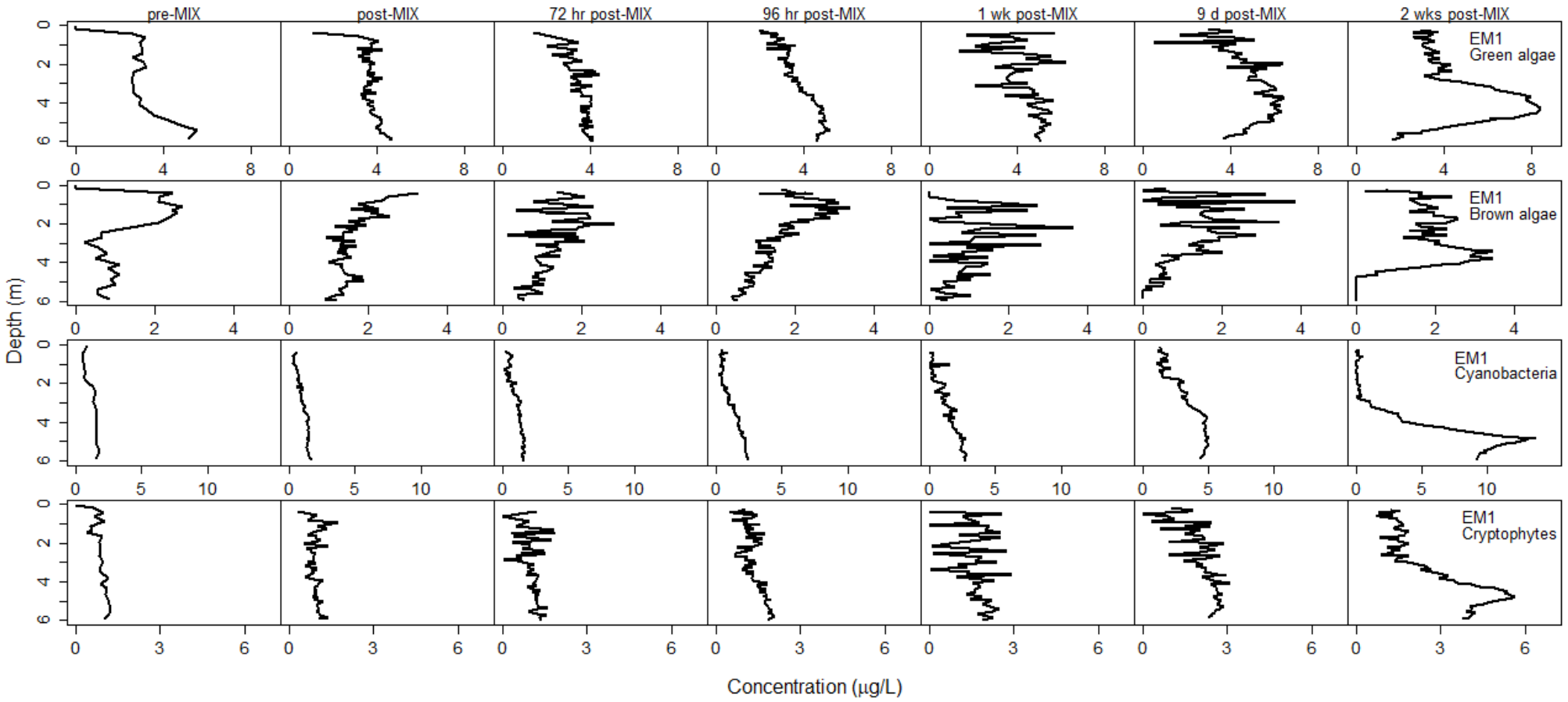

Figure S.4: Effect of the first mixing event (EM1) on the vertical distribution of phytoplankton spectral group biomass in the epilimnion of FCR. Pre-mix refers to 3-4 hours prior to the experimental mixing, and Post-mix refers to <1 hour after mixing.

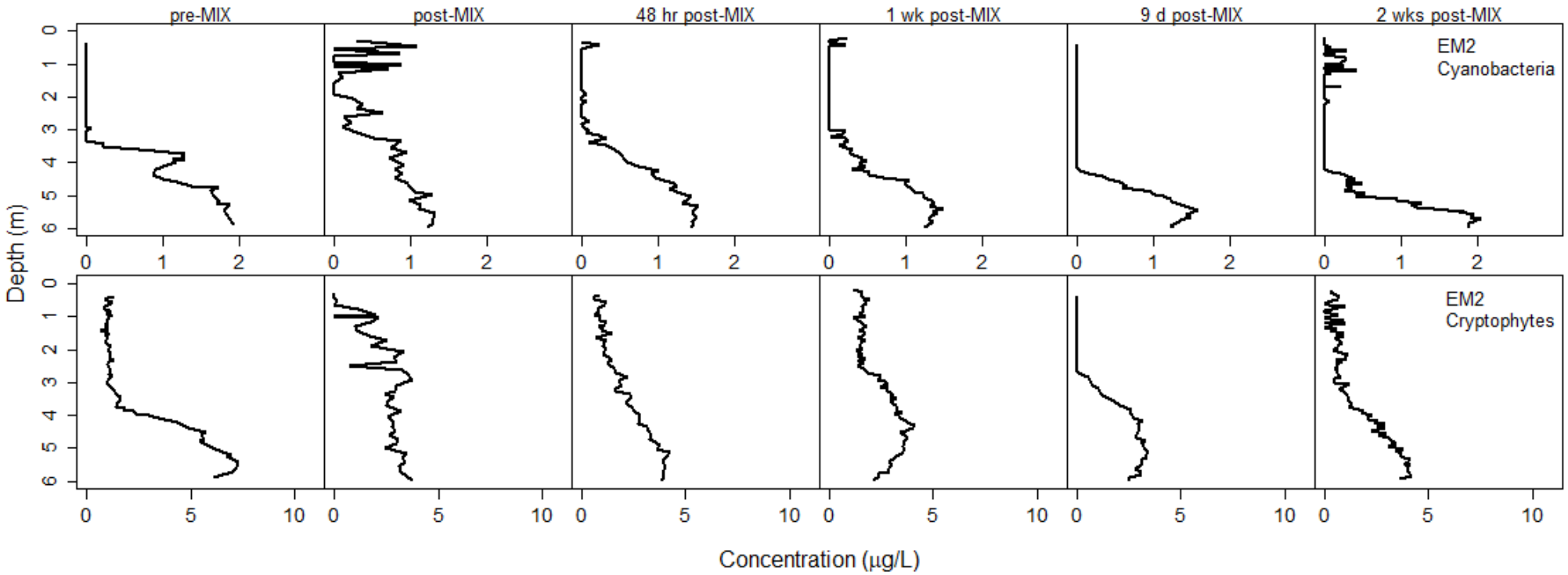

Figure S.5: Effect of the second mixing event (EM2) on distribution of phytoplankton spectral group biomass in the epilimnion of FCR. Pre-mix refers to 3-4 hours prior to the experimental mixing, and Post-mix refers to <1 hour after mixing.

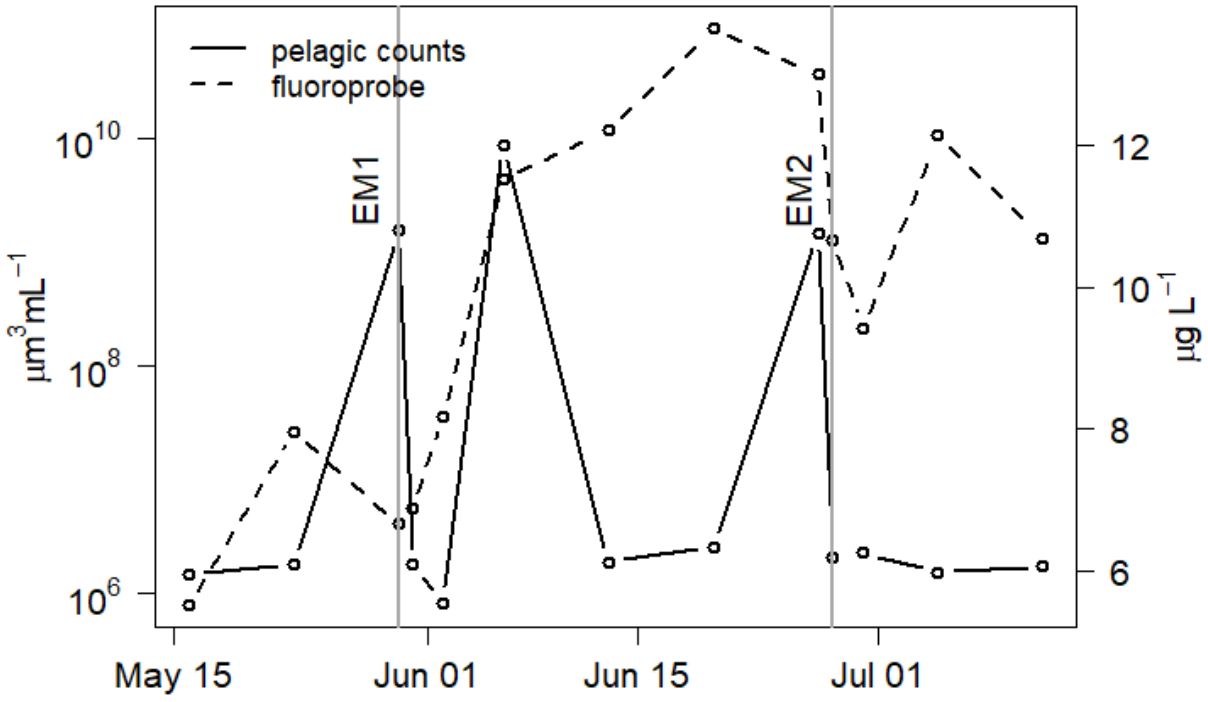

Figure S.6: Comparison of phytoplankton biovolume measured by microscopy (left y-axis) with mean biomass (right y-axis) as measured by the FluoroProbe across the treatment zone in Falling Creek Reservoir. Mixing events are denoted by vertical gray lines.

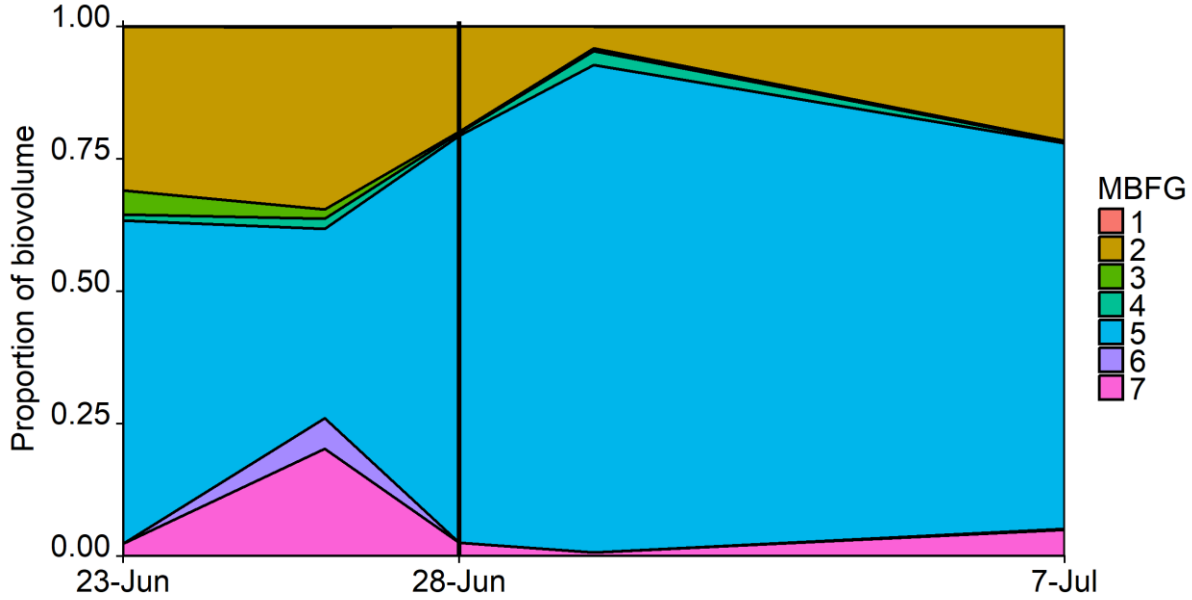

Figure S.7: Proportional biovolume of morphological-based functional groups (MBFGs) in the reference reservoir, Beaverdam Reservoir (BVR). The seven MBFGs are: 1-small, high SA:V cells; 2-small siliceous flagellates; 3-large, high SA:V filaments; 4-medium-sized, unspecialized cells; 5-medium/large flagellates; 6-non-flagellated siliceous cells; 7-large, mucilaginous, low SA:V colonies. EM2 is denoted by vertical black line.

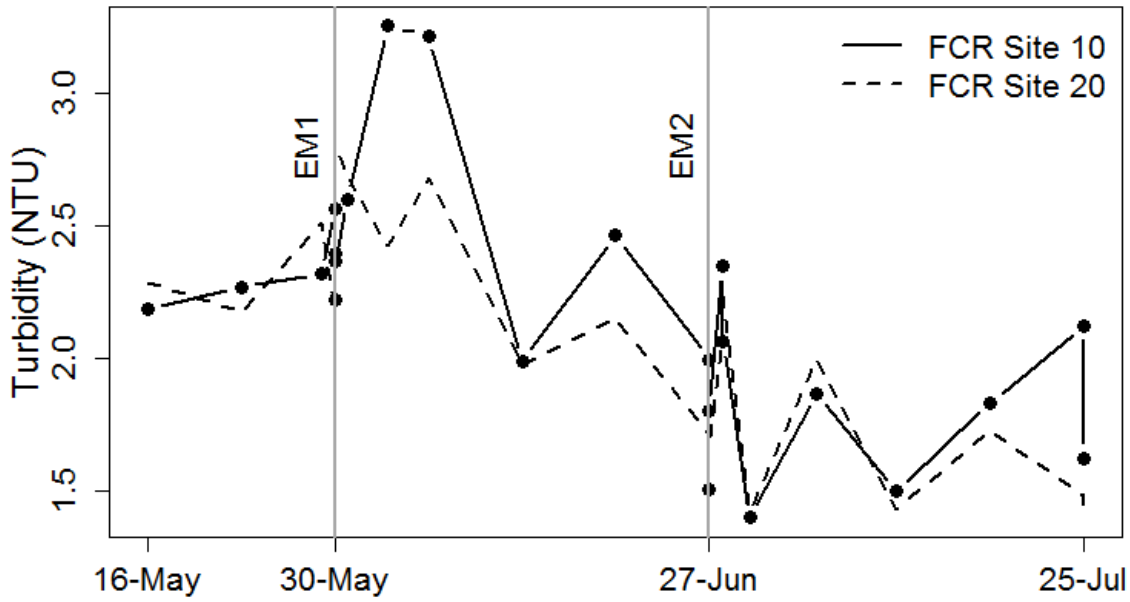

Figure S.8: Upstream turbidity in Falling Creek Reservoir (FCR) during the mixing experiment monitoring period. Site 10 and Site 20 are the two shallowest, most riverine sites in the reservoir (see Fig. 1). Mixing events are denoted by vertical gray lines.

References

Chen, S., Lei, C., Carey, C.C., Gantzer, P.A., Little, J.C., 2017. A coupled three-dimensional hydrodynamic model for predicting hypolimnetic oxygenation and epilimnetic mixing in a shallow eutrophic reservoir. Water Resour. Res. 52, 1–20. https://doi.org/10.1002/2016WR019279